UNIVERSITY OF PORTSMOUTH

School of Mechanical and Design Engineering

Coursework 1	Throttle Valve Assembly (3D CAD modelling)
Module:	Computer Aided Engineering (Product Realisation)
Course:	BEng (Hons) Mechanical and Manufacturing Engineering
Student ID:	UP2061013
Examiner:	………….
Date:	17/12/2025

Declaration

Declaration of Originality and Approval of Research Ethics

CW1 Title: Throttle Valve Assembly (3D CAD modelling)

Student ID: UP2061013

‘I certify that this is my own work, and it has not previously been submitted for any assessed qualification. I certify that the use of material from other sources has been properly and fully acknowledged in the text’.

Signed: UP2061013 Date: 17/12/2025

Contents

Introduction

This report documents the design and development of a throttle valve assembly using Creo PTC, in accordance with the coursework brief. The valve was modelled using metric units and developed with DFMA principles, including integration of standard machine elements to improve functionality, manufacturability, and cost effectiveness. The selected variant constraints were an internal bore diameter of 110 mm and a maximum operational pressure of 15 MPa, which were applied in the structural assessment of the valve body.

Last digit of Student ID Number	0	1	2	3	4	5	6	7	8	9
Valve internal diameter, mm	100	90	80	110	70	60	50	140	120	130
Maximum Operational Pressure, MPa	15	12	12	15	10	10	8	15	15	10

Figure 1: Variants of the coursework as stated within the brief

Outputs of this coursework include a fully constrained 3D assembly model, part models, application of casting relating design features (drafts, rounds and chamfers), material selection with mass and volume calculations for single and high-volume production, a comparative FEA of the valve body, an improved design iteration meeting a minimum safety factor, and BS8888 compliant technical drawings for the assembly and key components. The report is structured according to Tasks 1-10 as specified in the assessment brief.

1.0 Assembly Concept (Task 1)

Throttle valves are widely used in chemical, petroleum, water, and gas engineering applications, where performance directly influences the system efficiency and operational safety [1]. The throttle valve developed in this project is based on a constrained assembly of key components including the valve body, plate, shaft, bearings, and flanges.

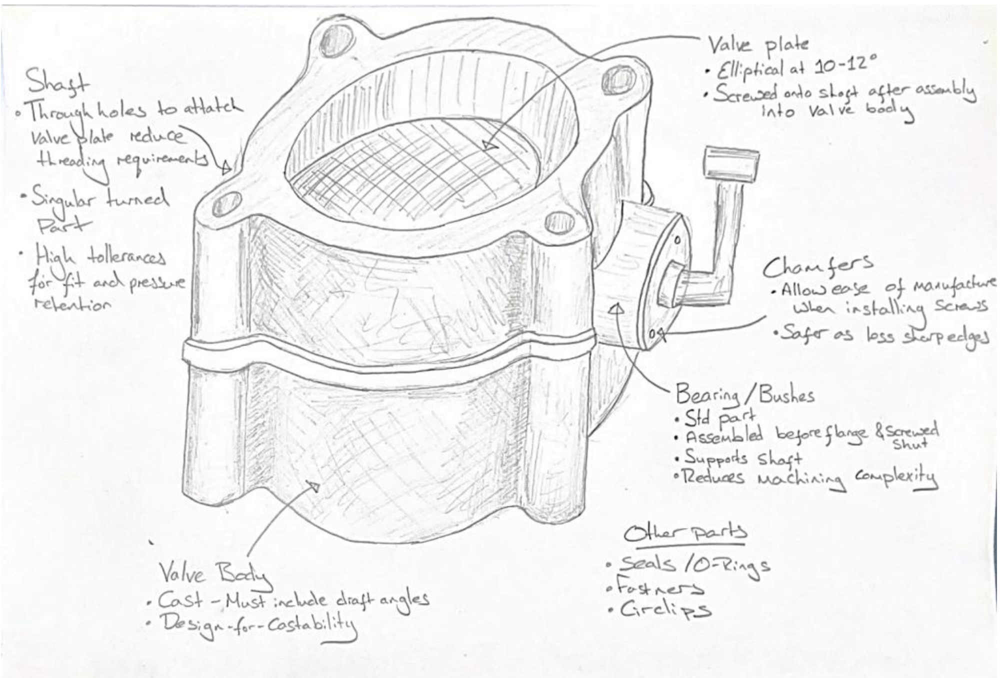

Figure 2: Initial Concept Sketch

2.0 Selection of the standard components (Task 2)

The selection of standard components is a key aspect of DFMA, influencing reliability, manufacturability, and cost efficiency. DFMA principles promote reduced part count, simplified assembly, and the use of standardised components produced to established ISO standards [2]. Accordingly, standard components were selected for this project where in house manufacture would not provide economic, quality, or lead-time advantages.

Part Name	Part Number	Supplier	Quantity
Flanged Bush	6659K4	McMaster-Carr	2
Ball Bearing	6656K105	McMaster-Carr	2
Thrust Bearing	2872T38	McMaster-Carr	1
Retaining Ring	95841A410	McMaster-Carr	1
M5 Socket-Head Screw	ISO14580-M5x10-5.8	Creo Directory	6
M5 Button-Head Screw	ISO-1-M5x22-8_8	Creo Directory	2
Washer	DINENISO7090-5	Creo Directory	2
Hexagonal Nut	ISO4032-M5-6	Creo Directory	2
Circlip	95841A410	McMaster-Carr	1
O-Ring	1302N104	McMaster-Carr	2

Table 1: Table of standard components and the quantities required per unit for assembly [3]

Threaded fasteners were selected for structural fastening due to their low cost, durability, and ease of assembly and disassembly [4]. A flanged bush was incorporated to support the rotating throttle shaft and maintain alignment under operational loading [5].

The built-in flange prevents axial migration, reducing the need for additional retention features and eliminating complex machining operations. Similarly, ball bearings were selected to deliver low friction rotation. Because the assembly also experiences axial loading, a dedicated thrust bearing was integrated to manage these forces and protect the radial bearings from premature wear. A circlip was included to "prevent the axial movements of parts" [6], specifically around the bearing stack. Its compatibility with standard groove dimensions allows rapid installation while maintaining precise axial positioning.

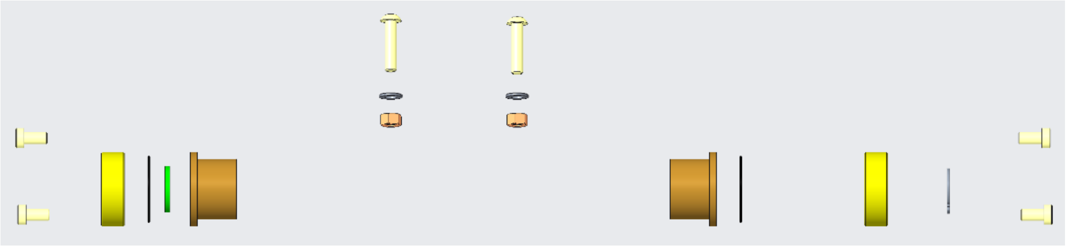

Figure 3: Exploded view of all standard parts within the assembly with designed components hidden

3.0 3D CAD Assembly and Verification (Task 3)

"One of the contributions of modern 3D CAD to accelerate the product development process is the ability to reuse and make alterations to existing models in an efficient and relatively easy manner" [7]. Key components (plate, body, and shaft) were modelled parametrically to enable rapid iteration and later dimensional updates to satisfy safety factor and FEA requirements.

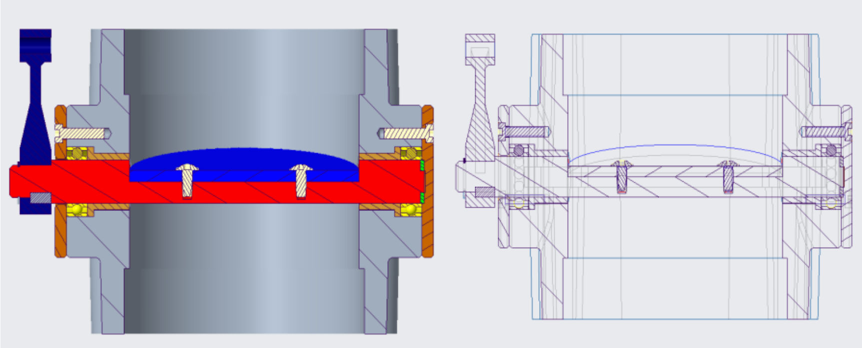

Figure 4: Cross sectional view of assembled part

The assembly comprises seven designed components and twenty standard components (27 total). Standard components were imported as STEP files (including sub-assemblies such as bearings) and fully constrained with the assembly.

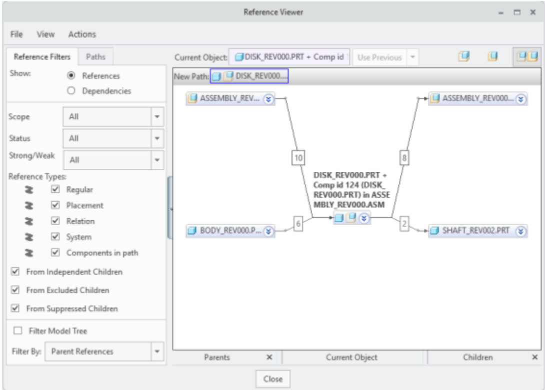

Figure 5: Reference viewer showing parent and child parts of parametric design

Functional verification was completed using a global interface analysis in Creo. No unintended interface was present between rotating and stationary components across the full range of motion; detected interfaces were limited to threaded fasteners and O-rings, where controlled overlap is required for fastening and pressure sealing. Clearances at shaft-support interfaces ensured free rotation with maintained concentric alignment. The valve plate and shaft orientation were verified at 11° about the shaft's axis to achieve full closure within the specified 10-12 ° range, satisfying the sealing requirement. All components were fully constrained without over constraint to maintain assembly stability.

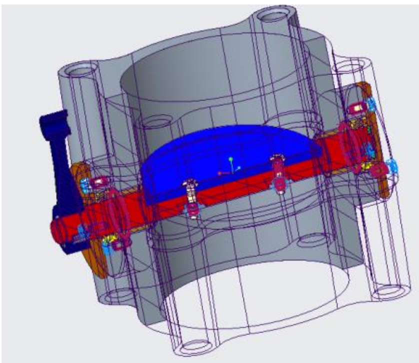

Figure 6: Global interference checks showing only O-rings and threaded parts containing interference

Interference Incident	Part 1	Part 2	Acceptable Part Inference
1	BODY_REV000	ISO14580-M5X10-5_8	OK
2	BODY_REV000	ISO14580-M5X10-5_8	OK
3	BODY_REV000	ISO14580-M5X10-5_8	OK
4	BODY_REV000	ISO14580-M5X10-4_8	OK
5	BODY_REV000	ISO14580-M5X10-4_8	OK
6	BODY_REV000	ISO14580-M5X10-4_8	OK
7	6659K44_OIL-EMBEDDED_FLANGED_SL	O_RING_REV000	OK
8	PRT002 (FLANGED_SL)	O_RING_REV000	OK
9	ISO7380-1-M5X22-8_8	ISO4032-M5-6	OK
10	DISK_REV000	ISO7380-1-M5X22-8_8	OK
11	SHAFT_REV002	ISO7380-1-M5X22-8_8	OK
12	ISO7380-1-M5X22-8_8	ISO4032-M5-6	OK

Table 2: Table of Interference Incidents

Localised interference between O-rings and their mating grooves was intentionally introduced to generate sealing pressure and prevent leakage under operational load conditions. Flange bolt preload provides the required clamp load to compress the O-rings and maintain a pressure-tight seal across the mating faces under operating conditions.

4.0 Drafts, rounds and chamfers (Task 4)

"A completely normal surface contacts the mould longer in the demoulding process than a surface with a draft angle, therefore, product draft angle must be considered" [8]. In Creo, draft angles are applied by tapering selected faces relative to a defined pull direction and neutral plane, producing the required mould release geometry.

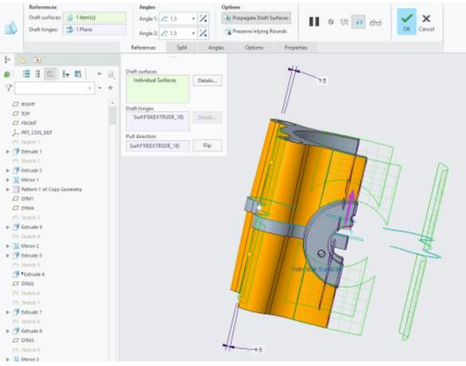

Figure 7: Creation of Draft Angles using Creo's Draft tool

Creo's Draft angle analysis tool was used to evaluate drafted faces relative to the mould pull direction using a colour coded display, verifying adequate draft for manufacturability and part release.

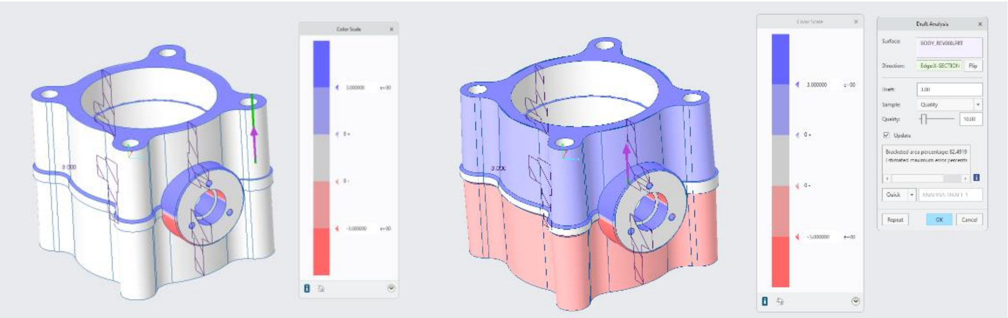

Figure 8: Draft analysis of Throttle Body; left and right images show before and after drafting respectively

For the throttle body, draft angles of 1.5° were applied to all external vertical faces in accordance with common gravity die casting practice. This ensured reliable demoulding while minimising dimensional deviation and preserving sealing performance and bore alignment.

Chamfers and rounds were applied to improve manufacturability, structural performance, and user safety. Rounds were used to reduce stress concentrations at corners, while chamfers were applied at pinch points and screw holes to assist assembly and handling. These features were implemented in Creo using the Round and Chamfer tools to ensure consistent transitions and adherence to design intent.

5.0 Material selection and mass calculation (Task 5)

Creo Part Name	Selected Material	Density (kg/m³)	Volume (m³)	Mass per Valve	Mass for 1x10⁶ Valves (kg)
BODY_REV000	AISI 1018 Carbon Steel [9]	7.87×10^{3}	1.08×10^{-3}	8.54	8.54×10^{6}
SHAFT_REV002	AISI 1045 Steel [10]	7.85×10^{3}	4.11×10^{-3}	0.323	3.23×10^{5}
DISK_REV000	Stainless Steel 304 [11]	8.00×10^{3}	4.82×10^{-3}	0.386	3.86×10^{5}
HANDLE_REV000	AISI 1018 Carbon Steel	7.87×10^{3}	1.65×10^{-3}	0.130	1.30×10^{5}

Table 3: Material Selection of Non-Standard Parts

Part Name (Material)	Material Justification
Throttle Body (AISI 1018 Carbon Steel)	Selected for its balance of yield strength, ductility, machinability and suitability for casting and machining operations.
Throttle Shaft (AISI 1045)	Higher strength steel selected to resist torsional and bending loads during valve actuation.
Valve Plate (Stainless Steel 304)	Corrosion-resistant material selected for durability at the sealing interface and exposure to airflow.
Actuation Arm (AISI 1018 Carbon Steel)	Cost-effective steel with sufficient strength for actuation loads and ease of manufacture.

Table 4: Material Selection of Non-Standard Parts Continued

Figure 9: Creo Information Window for parts discussed in Table 3+4

In addition to strength considerations, the selection of AISI 1018 CS was informed by its favourable balance of ductility, machinability, and availability. The material's relatively low carbon content improves toughness and reduces sensitivity to brittle fracture, which is advantageous for pressure containing components subjected to local stress concentrations. Furthermore, its widespread industrial use and compatibility with conventional machining processes support cost effective manufacture and dimensional control, reinforcing its suitability for the valve body application.

6.0 Valve body strength analysis and discussion (Task 6)

6.1 Analysis Setup and Assumptions

The valve body FEA was conducted to evaluate structural performance under the maximum operational pressure specified for the selected variant. A uniform internal pressure load of 15 MPa was applied to all internal bore surfaces, representing a conservative worst case operating condition.

Structural constraints were applied at the mounting faces to represent the bolted flange interfaces, preventing rigid-body motion while allowing realistic load transfer without artificially increasing model stiffness.

Material properties were assigned directly within Creo using published datasheet values, including Young’s modulus, Poisson’s ratio, density, and yield strength, ensuring consistency between structural analysis and mass calculations.

The safety factor was determined by comparing the maximum Von Mises stress with the material yield strength. A minimum safety factor of SF ≥ 2 was adopted to ensure elastic behaviour under operational loading and provide an adequate margin against yielding.

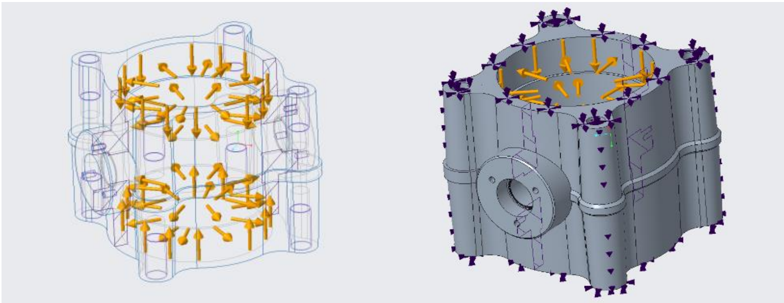

Figure 10: FEA Setup for all analysis within chapter 6 - Pressure = 15 MPa

6.2 FEA Results Summary and Comparison

A36 mild steel [12] was selected for the preliminary FEA due to its suitability for casting, resulting from good formability [13], as well as its high strength, toughness, and widespread industrial use [14]. Where ranges of material properties were available, lower bound values were selected to ensure conservative safety assesments.

<table>
<tr><td>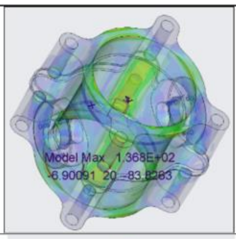
</td><td colspan="2">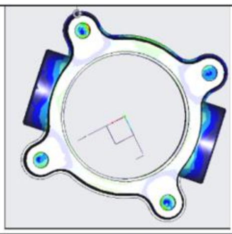</td><td>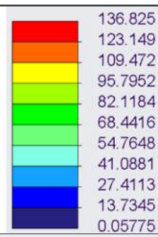
</td></tr>
<tr><td>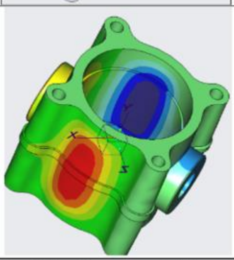</td><td colspan="2">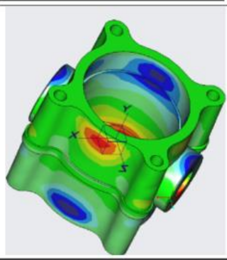</td><td>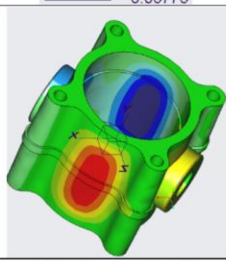</td></tr>
<tr><td>Max Displacement (X axis)</td><td colspan="2">Max Displacement (Y axis)</td><td>Max Displacement (Z axis)</td></tr>
<tr><td colspan="4">Total Maximum Displacement Magnitude: $2.45x10^{-2}$ mm</td></tr>
<tr><td>Elastic Limit</td><td>Maximum Von Mises Stress</td><td>Safety Factor</td><td>Part Mass</td></tr>
<tr><td>220 MPa</td><td>136.8 MPa</td><td>1.6</td><td>9.58 Kg</td></tr>
<tr><td colspan="4">SF Requirements met - No</td></tr>
</table>

Table 5: FEA Results #1 - A36 Mild Steel; No Geometric Changes

The second FEA revision changes to a more ductile material, AISI 1018 [9]. As no geometric changes were introduced between the first two analyses, displacement occurred at similar locations within the part.

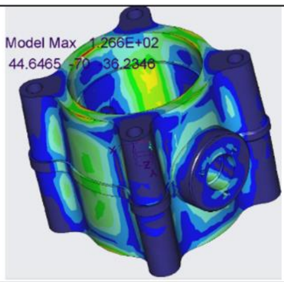		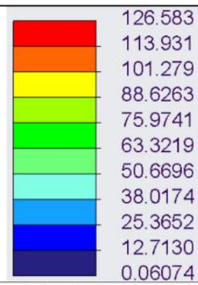	
Max Displacement (X axis)	Max Displacement (Y axis)	Max Displacement (Z axis)	
Recorded Value: 1.70×10^{-2} mm	Recorded Value: -3.69×10^{-3} mm	Recorded Value: -1.70×10^{-2} mm	
Total Maximum Displacement Magnitude: - 0.67μm			
Elastic Limit	Maximum Von Mises Stress	Safety Factor	Part Mass
370 MPa	126.6 MPa	2.95	9.61 kg
SF Requirements met - Yes			

Table 6: FEA Results #2 - AISI 1018 Carbon Steel; No Geometric Changes

A further analysis iteration was performed in which selected internal geometric features, including stepped bore transitions and threaded bolt hole shoulders, were simplified to create a more uniform internal geometry. The same material properties were retained to isolate the influence of geometric refinement on stress concentration and displacement behaviour. Displacement again occurred at similar locations within the part.

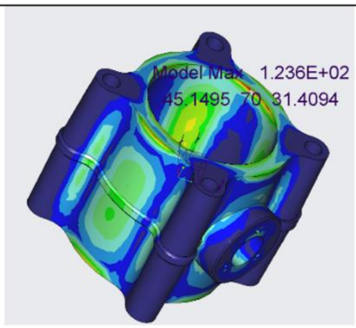		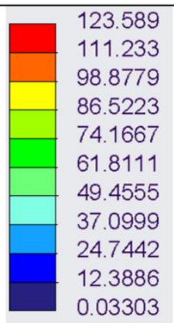	
Max Displacement (X axis)	Max Displacement (Y axis)	Max Displacement (Z axis)	
Recorded Value: 1.56×10^{-2} mm	Recorded Value: -3.24×10^{-3} mm	Recorded Value: -1.55×10^{-2} mm	
Total Maximum Displacement Magnitude: 2.19×10^{-2} mm			
Elastic Limit	Maximum Von Mises Stress	Safety Factor	Part Mass
370 MPa	123.6 MPa	2.99	9.75 kg
SF Requirements met - Yes			

Table 7: FEA Results #3 - AISI 1018 Carbon Steel; With Geometric Changes

6.3 Discussion of Results and Design Implications

Pressure retention within the assembled valve is achieved through a combination of controlled geometric interference at the O-ring sealing interfaces and the structural stiffness of the valve body under internal pressure loading. The FEA results indicate negligible global deformation, ensuring that sealing surfaces remain aligned during operation. Localised elastic deformation at the sealing interfaces contributes to effective contact pressure without exceeding material yield limits, supporting reliable pressure containment under the specified operating conditions.

The FEA results indicate that the maximum Von Mises stress is consistently localised at regions of geometric discontinuity, particularly around bolt holes and internal bore transitions, where abrupt changes in cross section cause stress concentration under internal pressure loading.

Comparison of the analysed materials shows that although the overall stress distribution remains similar, the resulting safety factor is strongly influenced by material yield strength. The use of AISI 1018 CS produces a significantly higher minimum safety factor than the initial mild steel analysis, demonstrating that material selection alone can improve the structural performance without geometric modification.

In all cases, the predicted displacements are small relative to the overall valve body dimensions, indicating negligible global deformation and no compromise to sealing alignment or functional performance under operational loading.

The consistency of stress localisation across all analysis iterations further supports the robustness of the load paths within the valve body, indicating that subsequent optimisation efforts could focus on mass reduction rather than fundamental structural redesign.

Based on these results, a valve body manufactured from AISI 1018 CS satisfies the elastic strength requirements for the specified operating pressure. Localised stress concentrations indicate further optimisation potential through targeted geometric refinement, which directly informed the mass reduction study presented in Task 7.

7.0 Improved Valve Body Design (Mass Reduction, SF ≥ 2) (Task 7)

Following the stress analysis presented in Task 6, a further design iteration was undertaken t reduce valve body mass, while maintaining a minimum safety factor of SF ≥ 2. Regions identified as low stress were selectively modified, while critical features including flange interfaces, bolt hole regions, sealing surfaces, and shaft support were preserved.

The overall body length between the outer end faces was reduced from 140 mm to 120 mm, targeting non-critical mid-body material only. The revised geometry was analysed under the same loading and constraint conditions as Task 6, with stress remaining localised in similar regions and no new stress concentrations introduced.

Creo Part / FEA Study	Description	Mass (kg)	Max Von Mises Stress (MPa)	Safety Factor
Body_Rev003	Stress-refined geometry	9.75	123.6	2.99
Body_Rev004_Mass_Reduction	Mass-reduced geometry (140 → 120 mm)	8.54	122.2	3.03

Table 8: Comparison of Valve Body Design Iterations

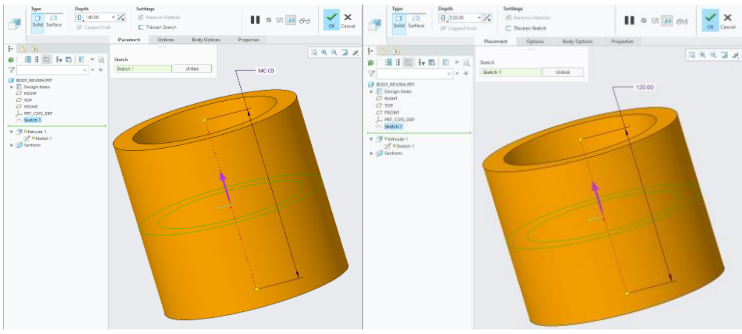

Figure 12: Valve Height Reduction

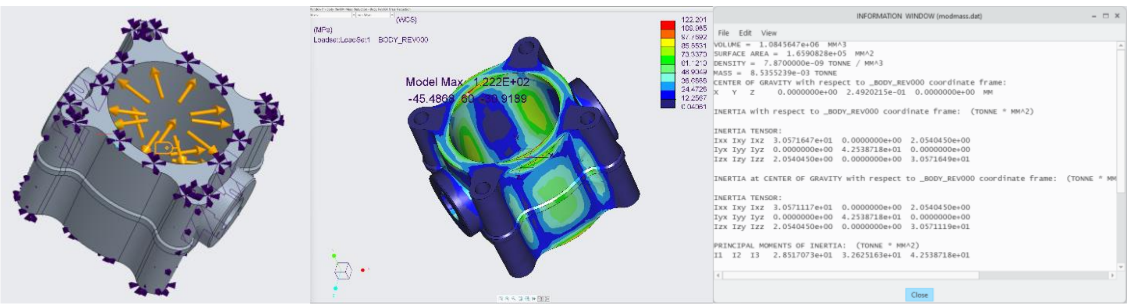

Figure 11: FEA Setup and Results of Valve Body Iterations

8.0 Assembly Drawings (BS 8888) (Task 8)

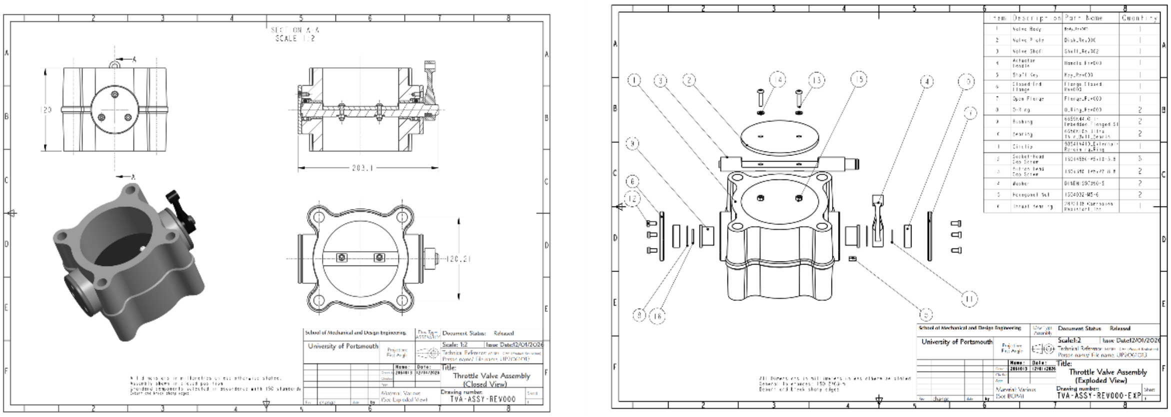

Figure 13: Throttle Valve Assembly (Closed View) Drawing + Throttle Valve Assembly (Exploded View) Drawing

An assembly drawing of the throttle valve was produced in accordance with BS8888 to communicate the spatial arrangement and functional relationships between components. The drawing includes a sectional view through the bore and shaft to clearly illustrate the positioning of the valve plate, shaft supports, and sealing features, together with a bill of materials identifying standard and-nonstandard components. This ensures the assembly intent and functional interfaces are clearly defined.

9.0 Detail Drawings: Selection of Fits and Tolerances (Task 9)

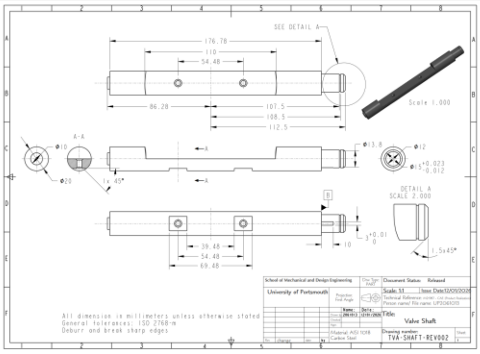

Figure 14:Shaft Handle Detailed Drawing (Non-Standard Part)

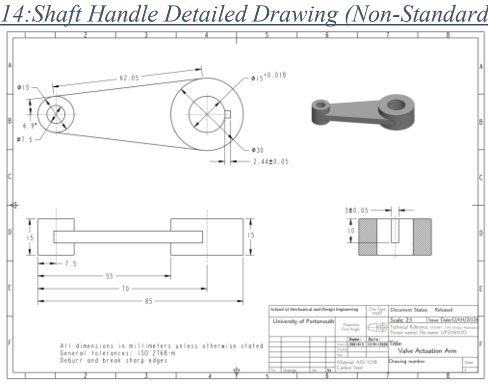

Figure 15: Valve Actuation Arm Detailed Drawing (Non-Standard Part)

The shaft and actuation arm drawings define manufacturing requirements through explicit tolerances and surface finish, in accordance with BS8888.

Conclusions

This coursework demonstrated the effective use of integrated 3D CAD software to support the full product realisation process, from concept development through detailed design, analysis, optimisation and technical documentation. Parametric modelling within Creo enabled efficient design iteration while maintaining design intent, significantly reducing rework during geometry refinement.

Constraint based assembly modelling proved critical in verifying functional intent. Fully constrained assemblies ensured correct alignment, concentricity and controlled motion, while interface and clearance checks identified potential assembly issues prior to manufacture, reducing downstream risks.

The integration of standard machine elements supported DFMA principles by reducing part count, simplifying assembly, and improving serviceability. However, reliance on standard CAD library components also highlights limitations, including assumed tolerances, nominal material properties, and idealised geometry that may not fully represent supplier variation.

CAD integrated FEA enabled rapid assessment of structural performance and provided a clear design analysis feedback loop. Stress and displacement results informed targeted geometric refinement, resulting in a mass reduced valve body while maintaining a safety factor exceeding the design requirement. Nevertheless, the analysis remained dependant on modelling assumptions such as boundary conditions and linear elastic behaviour, reinforcing that CAD based FEA is a decision support tool rather than a substitute for experimental validation.

Optimisation within the CAD environment required engineering judgement to balance performance, manufacturability, and reliability. Material removal was guided by stress distribution rather than minimising peak stress alone, ensuring functional interfaces and load paths were preserved.

Finally, the production of BS8888 compliant assembly and detail drawings demonstrated the role of CAD as a technical communication tool. Associative drawings ensured consistency between models and documentation, while the separation of assembly drawings (fit and functional intent) from detail drawings (manufacturing limits, tolerances, and surface finish) enabled unambiguous interpretation.

Overall, the project illustrates that while integrated CAD tools significantly enhance efficiency and analytical capability, robust product realisation still depends on critical evaluation, engineering principles, and realistic consideration of manufacturing variability.

While the analysis demonstrates adequate performance under static loading, experimental validation would be required to fully characterise fatigue behaviour and sealing performance under cyclic pressure conditions.

Appendix

Table of Figures

List of Tables

Table of Abbreviations

DFMA	Design for Manufacture
ISO	International Standards Organization
FEA	Finite Element Analysis
CS	Carbon Steel
mm	Millimetres
µm	Micrometres
kg	kilogram
MPa	Mega Pascals
AISI	American Iron and Steel Institute
CAD	Computer Aided Engineering
3D	Three Dimensional

References

[10] *AISI 1045 Steel, Quenched and Tempered to 450 HB*. (2025). Matweb.com. https://matweb.com/search/DataSheet.aspx?MatGUID=bbc93d88f424449ba85dbc06314080d2

[14] Ayoola, A. A., Babalola, R., Durodola, B. M., Alagbe, E. E., Agboola, O., & Adegbile, E. O. (2022). Corrosion inhibition of A36 mild steel in 0.5 M acid medium using waste citrus limonum peels. *Results in Engineering*, *15*(100490), 100490. https://doi.org/10.1016/j.rineng.2022.100490

[7] Camba, J. D., Contero, M., & Company, P. (2016). Parametric CAD modeling: An analysis of strategies for design reusability. *Computer-Aided Design*, *74*, 18–31. https://doi.org/10.1016/j.cad.2016.01.003

[4] Croccolo, D., Massimiliano De Agostinis, Fini, S., Muhammad Yasir Khan, Mele, M., & Giorgio Olmi. (2023). Optimization of Bolted Joints: A Literature Review. *Metals*, *13*(10), 1708–1708. https://doi.org/10.3390/met13101708

[5] Hrițuc, A., Slătineanu, L., Dodun, O., Nagîț, G., Coteață, M., Boca, M. A., & Ermolai, V. (2021). Sustainable Manufacture of Bearing Bushing Parts. *Sustainability*, *13*(19), 10777. https://doi.org/10.3390/su131910777

[6] Jing, B., Li, C., Shi, Y., & Li, C. (2023). Research on Mechanical Simulation Experiment and Assembly Technology for Large-size Circlip for Hole. *IEEE Xplore*, *5*, 123–128. https://doi.org/10.1109/asim62342.2023.00030

[8] Jong, W.-R., Li, T.-C., Chen, Y.-W., & Ting, Y.-H. (2017). Automatic Recognition and Construction of Draft Angle for Injection Mold Design. *Journal of Software Engineering and Applications*, *10*(01), 78–93. https://doi.org/10.4236/jsea.2017.101005

[2] Juniani, A. I., Singgih, M. L., & Karningsih, P. D. (2022). Design for Manufacturing, Assembly, and Reliability: An Integrated Framework for Product Redesign and Innovation. *Designs*, *6*(5), 88. https://doi.org/10.3390/designs6050088

[11] Matweb. (2024). *ASM Material Data Sheet*. Asm.matweb.com. https://asm.matweb.com/search/SpecificMaterial.asp?bassnum=mq304a

[9] *MatWeb - The Online Materials Information Resource*. (n.d.). Matweb.com. https://matweb.com/search/datasheet.aspx?MatGUID=e60983fcde914b278ceffebb946995e6

[13] McClements, D. (2025, Summer 9). *Low-Carbon Steel: Properties, Uses, and Types*. Thomas for Industry. https://www.thomasnet.com/articles/metals-metal-products/low-carbon-steel/?msockid=26455185eae6652f1b414746eb09649f

[3] *McMaster-Carr*. (2019). Mcmaster.com. https://www.mcmaster.com

[1] Rong, Z., Zhao, C., Qiyu, H., Pengbo, H., & Kuan, S. (2023). Simulation and Optimization Design of Tubular Throttle Valve Based on SolidWorks. *International Journal of Frontiers in Engineering Technology*, *5*(6). https://doi.org/10.25236/ijfet.2023.050602

[12] World Material. (2019, December 14). *ASTM A36 Steel Properties, Modulus of Elasticity, Yield Strength, Material Density, Hardness & Equivalent*. The World Material. https://www.theworldmaterial.com/astm-a36-steel/